IR Spectroscopic Characterization of the Buried Metal Interface of Metal-Molecule-Silicon Vertical Diodes

Christina A. Hacker*, Curt A. Richter*, Lee J. Richter†

*Semiconductor Electronics Division, Electronics and Electrical Engineering Laboratory,
†Surface and Microanalysis Science Division, Chemical Science and Technology Laboratory,
National Institute of Standards and Technology, Gaithersburg, MD 20899

Abstract. We have developed and utilized p-polarized backside reflection absorption infrared spectroscopy (pb-RAIRS) to examine dielectrics between silicon substrates and metallic overlayers. The technique has been used to investigate oxides, organic layers on oxides, and organic layers directly attached to silicon under Au, Al, and Ti. Simultaneous electrical test structures were prepared using a capacitor mask. Little interaction of the metal with oxides was observed in contrast to the observed interaction of the metal with the organic monolayers. The vibrational data were correlated with the electrical data to establish a cohesive understanding of the buried interface.

Keywords: infrared spectroscopy, organic monolayer, metal interface, RAIRS

INTRODUCTION

The buried interface between metals and thin dielectric films is critical to a diversity of technologies. Because interactions between dielectric and metal materials at this interface can lead to very different device properties (i.e., fermi level pinning, work function changes, etc.), a critical understanding of the reactions occurring at this interface is desired. The buried metal/dielectric interface is difficult to characterize *in-situ* since metal films become opaque to both optical and charge particle probes at thicknesses on the order of 10 nm. Therefore, the bulk of the interfacial analysis has been done either via the use of semi-transparent metal layers or via destructive analysis.

Due to the ability to prepare well-defined organic surfaces, the interface between metals and self-assembled monolayer (SAM) films has been extensively studied as a model for more complex interfaces.[1] More recently, the metal-monolayer-substrate system has gained interest due to opportunities in the molecular electronics arena. SAMs also hold promise as replacement diffusion barriers and dielectrics in conventional semiconductor device architectures[2] and are being explored as active components in molecular electronic schemes.[3] A key component necessary for the development of this latter application is the correlation of electrical performance with molecular structure. A diversity of interesting electrical behavior has been reported for molecular devices. In some, it has become clear that the behavior is universal; i.e., uncorrelated with the specifics of the molecular film, but associated with the measurement platform itself.[4,5]

We present the results of a straightforward optical measurement, p-polarized backside reflection absorption infrared spectroscopy (pb-RAIRS), that is applicable to any metal/dielectric/substrate system which utilizes an IR transparent substrate as shown in Figure 1. This method is advantageous since it is nondestructive and utilizes thick metal encapsulating the dielectric, which precludes sample degradation and allows for simultaneous fabrication of electrical devices. Special substrate shapes are not required, as in attenuated total internal reflectance, enabling the

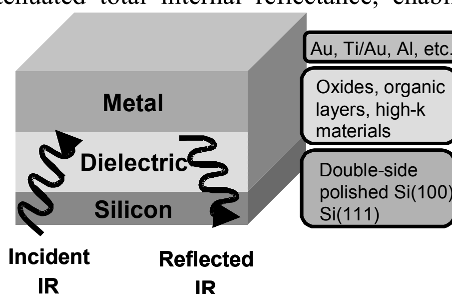

FIGURE 1. Schematic of backside reflection absorption infrared spectroscopy (bs-RAIRS) sample.

extension to acquisition of vibrational spectra under bias with optimized optics. We apply pb-RAIRS to interface characterization between vapor deposited top metal contacts (Al, Au, and Au with a Ti adhesion layer) and dielectric layers consisting of silicon oxides and alkane monolayers. The results are directly correlated with electrical data obtained from capacitor structures consisting of identically fabricated films.

EXPERIMENTAL

Two types of organic monolayers were studied: monolayers attached to silicon oxide (native and thermal) and monolayers attached directly to the silicon surface. Organic monolayers were prepared on double side polished Si(111) wafers (P doped, 8 Ω cm to 12 Ω cm). Octadecanol (OA) was attached directly to H-functionalized silicon[6] and octadecyltrichlorosilane (OTS) was attached to silicon oxide[7] as described previously. Briefly, Si-H substrates were placed in a 10 mmol/L alcohol solution (CH_2Cl_2) in an inert glove box and exposed to 254 nm irradiation to form Si-O-$(CH_2)_{17}CH_3$ surfaces. OTS was grown on oxide surfaces by 18 h immersion in 2 mmol/L hexadecane solution followed by extensive sonication and annealing to remove physisorbed material. Spectroscopic ellipsometry, contact angle, and transmission FTIR (Fourier transform infrared spectroscopy) were used to monitor the quality of the organic monolayers formed. The ellipsometric thickness indicates a slightly lower density for the directly attached films, compared to silanization, which has been attributed to packing constraints imposed by the Si lattice.[6]

Three top metal layers were deposited from physical evaporation sources: 200 nm of Al, 200 nm of Au, and 9 nm of Ti followed by 200 nm Au (Ti:Au) [8] as described elsewhere.[7] Blanket films were deposited on (≈15 mm x 15 mm) samples for FTIR characterization, while arrays of 150 µm diameter dots were deposited via a shadow mask for electrical characterization. Reference samples were created by deposition of the metals directly on the thermal and native oxide films and on H-Si. The alkane films and metal depositions were performed via batch processing, providing a high degree of reproducibility.

All IR spectra were recorded with a commercial FT instrument by using a liquid nitrogen cooled MCT (mercury cadmium telluride) detector at 8 cm^{-1} resolution. 512 scans were coadded for a total data acquisition time of ≈6.5 min. P-polarized Brewster angle (≈73.7°) transmission spectra were acquired with a custom-built sample holder. P-polarized, near-Brewster angle, backside reflection spectra were acquired with a commercial 80° reflection accessory. The actual reflection angle was determined to be ≈76.5°. For both measurements, wire grid polarizers, on either ZnSe or BaF_2 substrates, were used to define the polarization. Electrical capacitance-voltage (C-V) and DC-current-voltage (I-V) data were collected on samples directly after metallization using a commercial probe station.

RESULTS AND DISCUSSION

Oxide Samples

Shown in Figure 2 are transmission spectra acquired from a 3.5 nm thermal oxide and a 1.7 nm native oxide sample.[9] The dominant features in the oxide region are the Si-O-Si symmetric stretch (ν_{sym}) at ≈816 cm^{-1} and the Si-O-Si asymmetric TO phonon at 1066 cm^{-1} and LO phonon at 1262 cm^{-1}. The negative dip at 1107 cm^{-1} is an artifact due to miss-cancellation of the Si-O-Si stretch of bulk O impurities.[10] Also shown in Figure 2 are the reflection spectra obtained after Au, Al, and Ti:Au were evaporated on the respective oxide samples. The Si-O ν_{sym} and TO phonon are suppressed in the reflection spectrum compared to the transmission spectrum. This is due to the surface selection rule for the presence of the metal over layer causing the reflection spectrum to be dominated by the zz element of the film dielectric tensor. The transmission spectrum, due to refraction, is a nearly equal mix of the in-plane (xx, yy) and normal (zz) components.

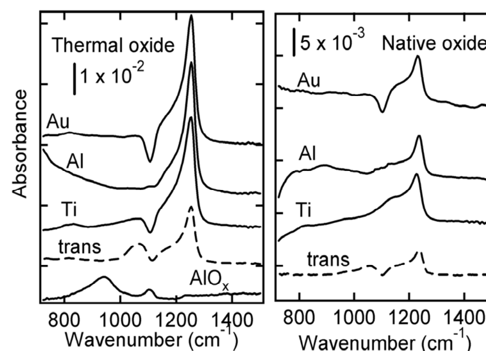

FIGURE 2. Transmission spectra (dotted line) obtained from clean oxide substrates. Reflection spectra obtained from Al, Au, and Ti deposited on the respective oxide. A spectra obtained from AlO_x on oxide is shown for comparison.

Also shown in Figure 2 is a spectrum obtained from a deliberately oxidized Al sample prepared by exposure of 2.5 nm of the Al to ambient conditions for ≈30 min prior to evaporation of 200 nm of Au. Comparison of the spectra obtained from the silicon oxide and AlO_x samples indicates that there is no observable metal oxide formation at this interface, consistent with earlier work.[11] Similar TiO_2 samples were made with no observable TiO vibrational stretches observed. Modeling and literature spectra indicate that TiO_2 features will initially appear at ≈820 cm^{-1} and be difficult to distinguish for thin layers. Overall, evaporation of Au, Al, and Ti do not dramatically affect the vibrational spectra obtained from native and thermal oxide surfaces.

Organic Monolayers

Shown in Figure 3 are p-polarized Brewster angle transmission spectra of the double side functionalized alkane monolayers on oxides. The spectra are referenced to a freshly prepared H-Si sample and agree with previous reports.[12,13] The dominant features in the CH stretch region are the methylene symmetric stretch (d+ near 2850 cm^{-1}) and asymmetric stretch (d- near 2920 cm^{-1}). These stretch frequencies can be used to characterize the degree of order of the alkane backbone.[14,15] The observed frequencies for OTS are consistent with a nearly all-trans, crystalline film.

Also shown in Figure 3 are the pb-RAIRS of the metallized films. In the low wavenumber region, the spectrum is dominated by the Si-O TO phonon. A weak feature at ≈930 cm^{-1} is observed for aluminum on OTS monolayers on both thermal and native oxide substrates that is attributed to aluminum oxide (Figure 2). No additional oxide features were observed for either the Au or Ti:Au films. In the CH stretch region, the vibrational spectra of the Al and Au metallized OTS films are very similar. The d- frequency shifts slightly to the blue upon metal deposition, indicative of slight disordering of the chains due to weak interactions with the metal. There is the appearance of a broad, weak feature in the Au spectrum at ≈2825 cm^{-1} attributed to a 'soft' methylene mode.[16] These modes indicate direct interaction of the CH_2 groups with the Au, suggestive of some metal penetration of the film. In contrast to the Al and Au results, the Ti:Au metallization causes significant changes in the vibrational spectra. The intensities of all CH bands are severely reduced, and the d- frequency appears at 2928 cm^{-1}, characteristic of a disordered liquid. The severe attenuation and disruption of the film is consistent with earlier studies of Ti on alkanes[17,18] and suggests chemical interaction, probably due to Ti carbide formation.

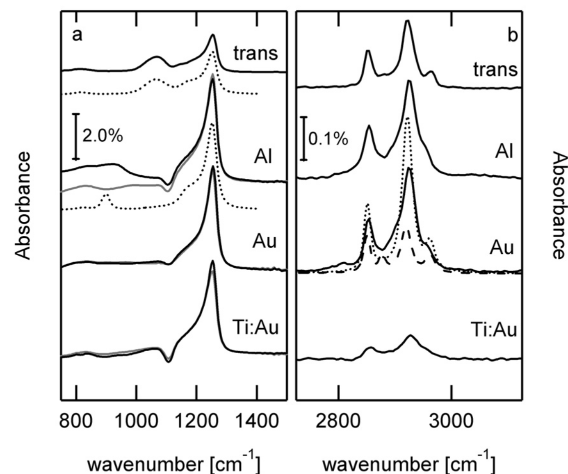

FIGURE 3. P-pol transmission and reflection IR spectra for OTS films assembled on thermal oxides. Gray lines: metal/oxide, Black lines: metal/OTS/oxide, broken lines: model spectra with isotropic (dotted) and biaxial (dashed) dielectric functions.

We have attempted to gain further insight into the degree of interaction between the metal and the film by quantitative modeling of the FTIR spectra. OTS films are known to consist of dense, all-trans aliphatic chains oriented near the surface normal.[19] This results in a highly uniaxial dielectric function ε for the alkane layer. We have developed a uniaxial model for the OTS films, based on fitting the p-pol and s-pol Brewster angle transmission spectra.[13] Shown in Fig. 3b as a dashed line is the expected reflection spectra if there is no perturbation of the film by the metal. Note that the unperturbed model does not well represent the observations. We have also simulated the reflection spectra, assuming the film has an isotropic dielectric function given by the average of the uniaxial film $\varepsilon_{iso}=(2\varepsilon_{\|}+\varepsilon_z)/3$. This is shown as the dotted line. The integrated intensity of the isotropic model is in fair agreement with the observed spectra.

In order to gain a further insight into devices, DC-current voltage (I-V) measurements were acquired on 150 um capacitor structures as shown in Figure 4. Controls of metal evaporated directly on the thermal oxide and native oxide substrates were performed. For both substrates, the presence of the OTS film significantly improves the leakage current for evaporated Al and Au, consistent with significant blocking of metal penetration by the alkane. The Ti:Au metalization results in less optimal behavior. While the OTS functionalization still blocks metal

penetration of the oxide, there is low resistance, suggestive of a thinner dielectric thickness. The dielectric thickness of the alkane films was estimated from the AC capacitance-voltage characteristics of the devices.[20] For the Ti/OTS devices, an OTS thickness of 0.7 nm was extracted. This is consistent with the pb-RAIRS (integrated intensity of the d+ and d- bands was 0.2 that of the isotropic reference spectrum implying ≈0.5 nm of remaining hydrocarbon) and supports the hypothesis of film consumption due to carbide formation. For the Al and Au devices, an OTS electrical thickness of 1.5 nm was determined. In the pb-RAIRS, the integrated d+ and d- intensities of the main features was ≈ 0.7 that of the isotropic reference (implying a thickness ≈ 1.8 nm), while the ratio of the soft d+ (2825 cm^{-1}) to the main d+ (2852 cm^{-1}) was 0.2. The electrical and optical data are most consistent with a thin (≈0.5 nm) combination region characterized by partial metal penetration into the film.

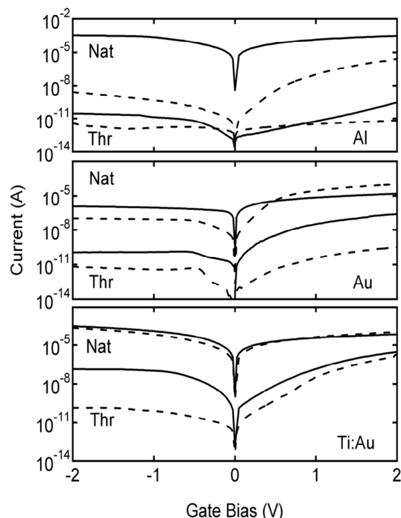

FIGURE 4. I-V characteristics for capacitors formed from the various metals on thin oxides and films. Key: black-metal/oxide, dashed-metal/molecule/oxide. Nat = native oxide and Thr = thermal oxide.

Shown in Figure 5 is the p-pol transmission IR spectrum for a C18 film directly attached to Si via UV promotion of the addition of octadecyl alcohol to H-terminated Si(111). Also shown in Fig. 5 are the pb-RAIRS spectra following the deposition of Al, Au, and Ti. In all three cases, there are no detectable hydrocarbon features in the spectra. Simulated spectra based on either a Bruggeman or Looyenya effective medium approximation for a film with 50 % metal fraction are shown in Fig. 5. Weak CH features are still present. This strongly suggests that the metals have displaced the OA derived films, severing the C-O-Si covalent linkage.

The displacement of the molecular film is consistent with the I-V characteristics, shown in Fig. 5. Reference devices, formed by direct deposition of the respective metal on the H-terminated surface, show the expected metal/semiconductor (M/S) behavior with the Au on n-type Si data exhibiting the most rectification (due to the larger work function of Au compared to Al and Ti). The changes in the I-V characteristics upon introduction of the directly attached film are very different than in the case of OTS/oxide. There is no evidence for significant blocking behavior in the presence of the molecular film. In fact, for Al and Ti, there is an *increase* in the reverse bias leakage, while, for Au, there is a slight decrease in the rectification and a decrease in the forward bias current. We suspect that the process by which the metal displaces the molecular film creates a metal/semiconductor interface that is less ideal than when the top metal is directly deposited on the pristine H-terminated Si surface. This causes a lowering of the Schottky barrier (with respect to that at the ideal metal/H-Si interface) which leads to the observed I-V curves having a greater reverse current leakage. C–V measurements (not-shown) are consistent with a direct M/Si interface and have no evidence for a dielectric barrier.

The displacement of the directly attached films is remarkable, when compared to the robust behavior of the silane-derived films. The R-O-Si linkage is slightly less stable than R-Si;[21] however, alcohol derived films are moderately stable in air, and aldehyde derived films are stable for 30 min in 60 °C water.[6] The displacement of the films cannot be attributed solely to film quality, as we have formed poor silane derived films (ellipsometric thickness: 1.8 nm, d-: 2925 cm^{-1}) and observed IR and I-V characteristics similar to those reported in Figs. 3 and 4.

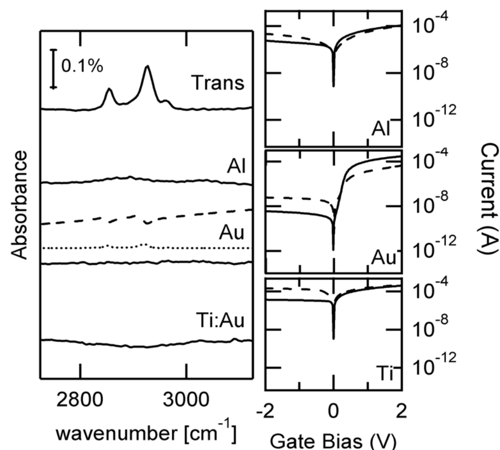

FIGURE 5. a) P-pol IR spectra of OA films directly attached to silicon. Broken lines are model spectra: Bruggeman (dotted) Looyenya (dashed). b) I-V data from H-Si (black) and OA-Si (dashed) capacitors.

Very little electrical characterization has been performed on directly attached films. In an earlier report, NIST presented C-V characterization of vapor deposited Al top contact, octadecyl alcohol derived films[22] The observed yield for blocking devices was extremely low. This is consistent with displacement of the molecules in the majority of the devices. C-V measurements have also been reported for vapor deposited Al on octadecene derived films,[23] and for Hg drop electrodes on dodecene functionalized surfaces.[24] The high surface tension of the Hg drop likely inhibits the metal film interaction and subsequent displacement. It is unclear the origin of the widely disparate results for Al/OA reported here and Al/octadecene reported in Ref 23. At a minimum, it indicates that the performance of directly attached films is highly variable.

CONCLUSIONS

Application of a novel backside infrared technique to samples of interest for molecular electronics is demonstrated. Vibrational spectra were obtained and analyzed from organic monolayers and oxide surfaces to investigate the buried interface between an organic monolayer and an evaporated metal. The results obtained from the vibrational spectroscopy were correlated with the results obtained from electrical measurements of the same samples. There was no observable interaction between evaporated metal and the native or thermal oxide surfaces. The interface for the organic monolayers differed depending on the substrate. The monolayers on oxide had little interaction with gold and aluminum while titanium tended to digest the aliphatic chain. Conversely, monolayers directly attached to silicon were displaced by all of the metals in this study. Both techniques are in good agreement and demonstrate the applicability of infrared spectroscopy for investigation of buried interfaces.

ACKNOWLEDGMENTS

We wish to thank S. Szeih for assistance in preparation of the OTS films, S. Hsu for use of the clean room facilities, and O. Kirillov for device preparation.

REFERENCES

1. F. Schreiber, *Progress in Surf. Sci.,* **65**, 151-256 (2000).
2. C. Boulas, J.V. Davidovits, F. Rondelez, and D. Vuillaume, *Phys. Rev. Lett.* **76**, 4797-4800 (1996).
3. C.R. Kagan and M.A. Ratner, *MRS Bulletin* **29,** 376-381(2004); M.C. Hersham and R.G. Reifenberger, *ibid*, 385-390; A. Ghosh, P. Damle, S. Datta, and A. Nitzan, *ibid*, 391-395; J.G. Kushmerick, D.L. Allara, T.E. Mallouk, and T.S. Mayer, *ibid*, 396-402.
4. D.R. Stewart, D.A.A. Ohlberg, P.A. Beck, Y. Chen, R.S. Williams, J.O. Jeppesen, K.A. Nielson, and J.F. Stoddart, *Nano Lett.* **4**, 133-136 (2004).
5. C.A. Richter, D.R. Stewart, D.A.A. Ohlberg, and R.S. Williams, *Appl. Phys. A*, accepted (2005).
6. C.A. Hacker, K.A. Anderson, L.J. Richter, and C.A. Richter, *Langmuir* **21**, 882-889 (2005).
7. C.A. Richter, C.A. Hacker, and L.J. Richter, *Nano Lett.*, submitted.
8. Thicknesses are nominal, based on a quartz crystal micro balance monitor.
9. Double-side polished Si(111) (P doped, 8 ohm cm to 12 ohm cm) wafers were SC1 cleaned. The 3.5 nm thermal oxide was grown at 800 ºC in dry-O_2 with a 30 min densification anneal in N_2 at 1000 ºC. Native oxide samples (1.7 nm thick) are chemically formed by an RCA clean further improved by a 30 min treatment in a commercial UV-ozone cleaner.
10. J.R. Ferraro and K. Krishnan, *Practical Fourier Transform Infrared Spectroscopy*, Academic Press, San Diego, 1990, Chpt. 6.
11. B. Brixner, *J. Opt. Soc. Am.* **55**, 1205 (1965).
12. A. Bierhals, A.G. Aberle, and R. Hezel, *J. Appl. Phys.* **83**, 1371-1378 (1998).
13. P. Harder, K. Bierbaum, Ch. Woell, M. Grunze, S. Heid, and F. Effenberger, *Langmuir* **13**, 445-454 (1997).
14. R.A. MacPhail, H.L. Strauss, R.G. Snyder, and C.A. Elliger, *J. Phys. Chem.* **88**, 334-341 (1984).
15. R.G. Snyder, H.L. Strauss, and C.A. Elliger, *J. Phys. Chem.* **86**, 5145-5150 (1982).
16. M. Yamamoto, Y. Sakurai, Y. Hosoi, H. Ishii, E. Ito, K. Kajikawa, Y. Ouchi, and K. Seki, *Surf. Sci.* **427**, 388-392 (1999) and references therein.
17. K. Konstadinidis, P. Zhanf, R.L. Opila, and D.L. Allara, *Surf. Sci.* **338**, 300-312 (1995).
18. B. de Boer, M.M. Frank, Y.J. Chabal, W. Jiang, E. Garfunkel, and Z. Bao , *Langmuir* **20**, 1539-1542 (2004).
19. A.N. Parikh, D.L. Allara, I.B. Azouz, and F. Rondelez, *J. Phys. Chem.* **98**, 7577-7590 (1994).
20. The capacitance of the oxide and alkane were added in parallel based on assumed dielectric constants of 3.9 and 2.5 for the oxide and alkane, respectively.
21. J.A. Haber and N.S. Lewis, *J. Phys. Chem. B* **106**, 3639-3656 (2002).
22. C.A. Richter, C.A. Hacker, L.J. Richter, and E.M. Vogel, *Sol. St. Electron.* **48**, 1747-1752 (2004).
23. S. Kar, C. Miramond, and V. Vuillaume, *Appl. Phys. Lett.* **78**, 1288-1291 (2001).
24. Y.-J. Liu and H.-Z. Yu, *ChemPhysChem* **4**, 335-342 (2003).